Journal of Materials Chemistry

Cite this: J. Mater. Chem., 2012, 22, 3340

www.rsc.org/materials

PAPER

Light sensitive antiferroelectric achiral copolymers

Eduardo Artuto Soto-Bustamante,*[a] Carmen Mabel González-Henríquez,[a] Rafael Orlando Vergara-Toloza[b] and Wolfgang Haase[c]

Received 31st May 2011, Accepted 4th November 2011
DOI: 10.1039/c1jm12431e

Five copolymers were prepared by polymerization of azo-benzene methacrylate monomers in solution using AIBN as initiator. The mesophases were observed by a polarizing light microscope which showed tilted smectic C phases for almost all samples. One of them shows just one orthogonal smectic A_2 phase. The X-ray diffraction patterns reveal the existence of bilayer smectic C_2 mesophases. The spontaneous polarization and pyroelectric response are reported showing an antiferroelectric behaviour for three of the copolymers. The polar phase has to do with a preferable arrangement of side chains in a syndiotactic fashion, which promotes the formation of anticlinicity in the polymer net. We probe that it is possible to induce orientation of the chromophores subjected to irradiation with UV/Vis light and that it is proportional to the amount of monomers without the OH group within the copolymers. This is so far a unique manifestation of polar ordering due to the syndiotactic lateral distribution of mesogens bearing an OH group in a tilted smectic C_2 phase.

Introduction

Ferroelectricity involving a complex interplay of dielectric and elastic behaviour in highly non-linear systems is as much an art as a science. It is a very unusual phenomenon well described in ceramics since the middle of the 20th century, and that was reinforced in the seventies when Meyer predicted and described their existence in tilted smectic C chiral liquid crystals, a so called helielectric phenomenon.[1]

The electrostatic interaction, hydrogen bonding interactions[2–4] and the non-covalent forces play a very important role in the mesomorphic properties and in the electric behaviour of liquid crystalline compounds. Of great interest is the fact that they can exhibit a spontaneous electric polarization showing a ferro and piezoelectric response.[5–11] All these properties are related to the deformations that are produced within the system when an electric field is applied on the material.

On the other hand, the ferroelectric polymer poly(vinylidene fluoride) PVDF has been investigated extensively, since it exhibits a large spontaneous polarization and memory effect, whose principal property is the easy fabrication of thin films. Also its copolymer P(VDF-TrFE) has the same characteristics, allowing them to be used as transducers, sensors, *etc.*[12,13]

To find new systems that can exhibit ferro or antiferroelectric properties is not an easy task. In our previous studies we have described the synthesis of Schiff base composites and the physical and electric properties of these compounds.[14–16] We also extend these studies to analogous molecules but incorporating azo units in the core (N=N) instead of the –CH=N– bond, always with a hydroxyl group in the aromatic part.[17] Some of these composites exhibit a very broad smectic C phase which is related to the electric signal and value of spontaneous polarization. They evidenced typical antiferroelectric polarization hysteresis loops in the mesophase, showing bilayer smectic C_2 mesophases with some interdigitation grade at the layer interface in a broad temperature range. Surprisingly composites of a similar structure developed pyroelectricity but not switchable states.

In this paper, we report the first copolymer system consisting of azo-benzene mesogens that are able to build up a polar structure due to hydrogen bridges between the net consisting of tilted mesogens. The tacticity of side chain in the polymerization process must play an important role in the observed phenomena, being so far the first example of an achiral copolymeric system capable to orient dipoles that remains thermodynamically stable with time. The chemical structure is shown in Fig. 1.

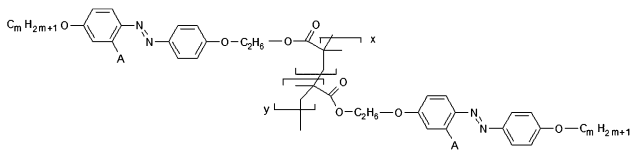

Fig. 1 The chemical structure of the copolymers CP(O)*m*-(O)*m*: A = H, *m* = 12(12), *m* = 8(8); A = OH, *m* = 12 (O12), *m* = 8 (O8).

[a]*Universidad de Chile, Facultad de Ciencias Químicas y Farmacéuticas, SergioLivingstone 1007, Independencia, Santiago, Chile. E-mail: esoto@ciq.uchile.cl; Fax: +562 9782868; Tel: +562 9782898*
[b]*Beam Engineering for Advanced Measurements Co., 809 S. Orlando Ave., Suite I, Winter Park, Florida, USA. E-mail: raftover@gmail.com; Fax: +1407 629 0460; Tel: +1407 629 1282*
[c]*Technische Universität Darmstadt, Petersenstr. 20, 64287 Darmstadt, Germany. E-mail: haase@chemie.tu-darmstadt.de; Fax: +49 6151 16 4924; Tel: +49 6151 16 3398*

The acronyms used CP(O)*m*-(O)*m* indicate the presence of a methacrylic like copolymer, linked through six methylene units as spacers adjacent to the aromatic group (CP). The aromatic group consists of two phenyl rings linked through a nitrogen double bond or azo group in the *para* position, where the nearest phenyl ring to the spacer may (O) or may not contain a hydroxyl group in the *meta* position. The aromatic group possesses, in its *para* position, an alkoxy chain with octyl and dodecyloxy units ($m = 8$ and $m = 12$).

Results and discussion

1.1 Polarized light microscopy

All copolymers were studied by polarized light microscopy. Characteristic textures for the SmC_2 phase for the CP8-12 and CPO12-8 copolymers are shown in Fig. 2a and 2b. In this figure a typical Schlieren texture obtained for heating at 139 °C and 140 °C is present, where the presence of singularities possessing four brushes with $s = \pm 1$ are identified. This kind of transition often results in an enhanced dipole–dipole interaction, leading to the formation of a more ordered smectic C phase that is related to the physical properties of the compounds. On the other hand, the CPO8-12 shows a smectic A_2 phase (see Fig. 2c) similar to the PO8-12 composite (PM6OA8-M6A12 33% of M6OA8 monomer mixed with 66% of PM6OA8 polymer) as described in previous publications.[17] The textures obtained using polarized light microscopy showed a perfect system of Dupin cyclides characteristic for the focal conic smectic A phase.

1.2 Differential scanning calorimetry

The phase transition temperatures and the corresponding enthalpies for the investigated copolymers obtained by DTA are summarized in Table 1. All the compounds reveal a clearing point between 160 and 167 °C by heating. The thermograms showed one peak by cooling and also by heating, related to the change from the liquid crystalline to the isotropic state and *vice versa*. All copolymers had comparable glass transition temperatures (T_g) upon heating to that showed for their polymers, from 71 °C to 84 °C. These data are obtained from the first scanning by heating at 4 °C min^{-1} rate.

The glass transition temperature (T_g) is dependent on the nature of the polymers backbone rigidity of the mesogenic group and the chemical composition of the copolymers. We could suppose that the monomer 12 within CPO12-12 and CPO8-12 respectively, gives flexibility to the system acted as a diluent, causing a decrease in the temperature. The phase transition temperature measurements of CP8-12 indicate the fact that a flexible copolymer backbone and a long flexible spacer tended to lead to a low glass transition temperature as well as a wide mesophase temperature range, which can be attributed to the molecular structure. On the other hand, when the percentage of monomer O12 within the system is slightly smaller than the monomer 8 in 44 : 56 ratios respectively for the CPO12-8 copolymer, the glass transition is increased considerably with respect to the other compounds.

1.3 Gel permeation chromatography

Table 2 summarizes the molecular weight characterization for three of the studied samples which correspond to the electroactive samples. The other samples CPO8-12 and CP8-12 possess comparable clearing point temperatures and glass transition temperatures (see Table 1). Then we may expect a similar behaviour on their molar mass distributions. No traces of monomer or oligomer fractions in the samples were detected in the chromatograms. The molecular weight relationship between different molecular weights was as expected: $\overline{M_{z+1}} > \overline{M_z} > \overline{M_w} > \overline{M_n}$. The molecular weights of polymers fall between 26 000 Da and 68 000 Da approximately. This fact together with a quite reasonable polymer dispersion index ($PDI = M_w/M_n$) ranging from 3.27 to 3.53, reflects the polymeric nature of the freshly polymerized samples.

1.4 X-Ray diffractometry

The X-ray diffractograms obtained for the mesophase of these compounds are show in Fig. 3. The diffraction showed two reflections in the small angle region. These reflections correspond to *d*001 and *d*002. The presence of theses peaks, together with the temperature dependence of the interlayer distance supports the existence of a smectic phase in the samples. The first reflections are related with the molecule length (see Fig. 4) which implies bilayer arrangement of side-chain mesogenic units in smectic planes, with a certain degree of interdigitation at the interface. The broad peaks in the wide angle region permit us to calculate

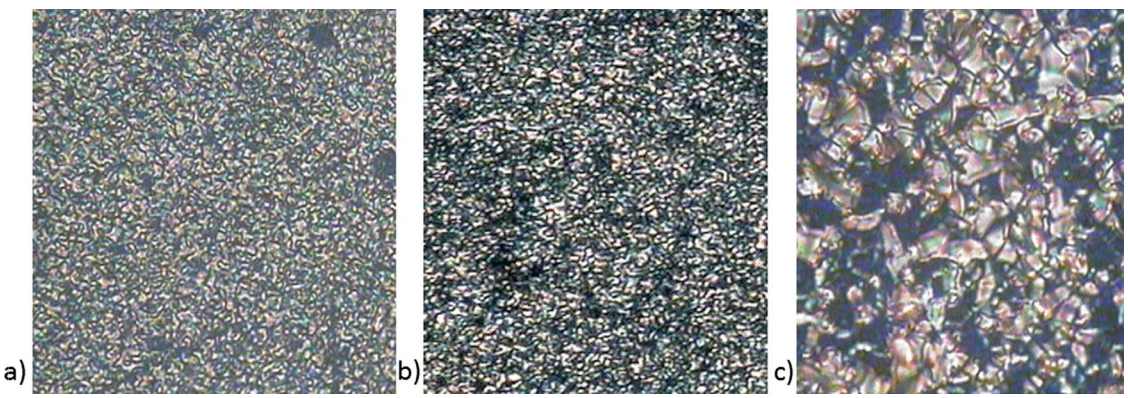

Fig. 2 Representative texture: a) CP8-12, $T = 139$ °C, SmC_2; b) CPO12-8, $T = 140$ °C, SmC_2; c) CPO8-12, $T = 92.7$ °C, SmA_2.

Table 1 Heating and cooling scans obtained by DTA for the investigated copolymers

Copolymer	Heating °C (J g^{-1})	Cooling °C (J g^{-1})
CPO12-8	g-83.5-SmC_2-167.0(16.4)-I	I-161.7(−10.7)-SmC_2-(ND[a])-C
CPO12-12	g-73.8-SmC_2-162.6(24.0)-I	I-153.7(−15.6)-SmC_2-(ND[a])-C
CPO12-O8	g-73.9-SmC_2-163.7(34.5)-I	I-155.3(−18.1)-SmC_2-(ND[a])-C
CPO8-12	g-74.1-SmA_2-160.8(16.4)-I	I-152.9(−9.26)-SmA_2-(ND[a])-C
CP8-12	g-71.2-SmC_2-167.0(15.5)-I	I-162.0(−10.1)-SmC_2-(ND[a])-C

[a] Not determined.

Table 2 Molecular weight of copolymers LCs used in this study

Copolymer	$\overline{M_n}$	$\overline{M_w}$	$\overline{M_z}$	$\overline{M_{z+1}}$	PDI
CPO12-8	16 422	58 037	112 473	140 729	3.53
CPO12-O8	19 444	67 931	121 153	146 025	3.49
CPO12-12	8 214	26 849	83 555	128 222	3.27

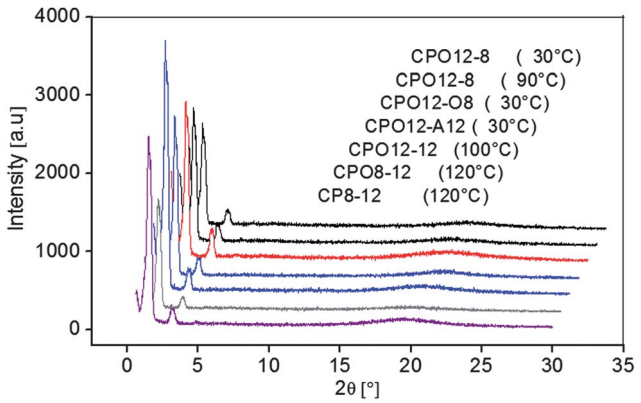

Fig. 3 X-Ray diffraction patterns at different temperatures.

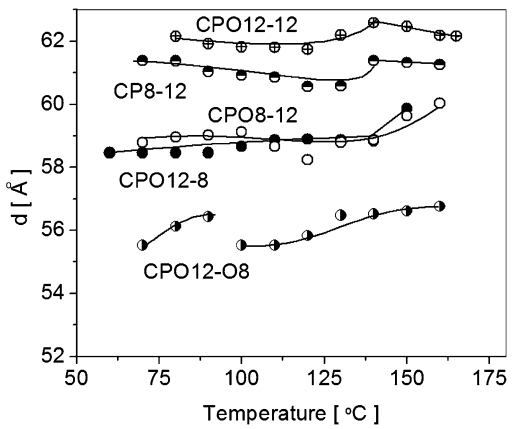

Fig. 4 The temperature dependence on cooling for the interlayer distance.

the average intermolecular distance D within the smectic layer; these values vary between $2\theta = 20.48$–19.90 with 4.33–4.45 Å at 30 °C. Thus molecular packing within the smectic layers must be considered as liquid-like.

Fig. 4 represents the interlayer distance against temperature for the copolymers showing SmC_2 phases. For simplicity, copolymer CPO8-12 possessing a SmA_2 phase was not included. This sample shows a monotonic trend of d-values at about 58.8 Å. For the other 4 samples, we deal with three different behaviours. For the copolymers CPO12-12, CP8-12 and CPO12-8 the temperature variation of the first order reflection in the mesophase behaves abnormally at high temperatures with an instability not noticed in the thermograms. This instability can be understood as a second order phase transition. Probably there is some degree of interdigitation of the smectic C_2 phase which reduces the values of the distance between layers at lower temperatures. We have noticed this abnormal behaviour in our previous work, in Schiff bases[18] and also azo-containing composites.[19] This situation is not seen for the CPO12-O8 sample probably due to the hydroxyl group present in each one of the monomeric units in the copolymer, which impart rigidity and stability to the system. At a low enough temperature, (about 90 °C), the abrupt change in the interlayer distance must be related with the glass transition process of the system, observed by DTA in the first scanning accompanied by heating (see Table 1).

Finally a third type of behaviour is shown for the copolymer CPO8-12. This sample shows a characteristic texture of an orthogonal smectic A phase. Therefore the interlayer distance resembles a smectic A_2 phase with a certain degree of interdigitation.

All the copolymers presented an interlayer distance smaller than twice the length of the side group, which is typical for a smectic C_2 phase. A strong evidence for the existence of a tilted bilayered smectic C phase in the new copolymers is due to the pyroelectric response observed in copolymers CPO12-12, CPO12-8 and CPO12-O8 (see Fig. 5).

The greater value of interlayer distance is shown for CPO12-12 with an average of $d = 62$ Å, related with the 12 carbon atoms in the terminal aliphatic chains. This behaviour is similar for the CP8-12 ($d = 61$ Å), due to the same reason. For CPO12-12 the O12 content was estimated at 36% from the signal ratio for the protons at about 6.40 and 6.60 ppm (2H) present in O12, compared with the signal at about 7.25 ppm (4H) of the second benzene ring just present in monomer 12. The CPO12-8 and CPO8-12 have an interlayer distance about 58.5 and 59 Å. This agrees well with the percentages of each component in the copolymer which is similar in both cases and estimated at 44% and 46% for the O12 and O8 fraction from ^{1}H-NMR. Finally, the CPO12-O8 has a minor interlayer distance of 55.5 Å. Here the O8 monomer content is bigger within the copolymer which reflects the decrease of the experimental interlayer distance.

The molecule length L was calculated using HF and MP2 methods (GAMESS program package) using a 631-G* basis set for the monomers previously studied which was 38.76 Å for

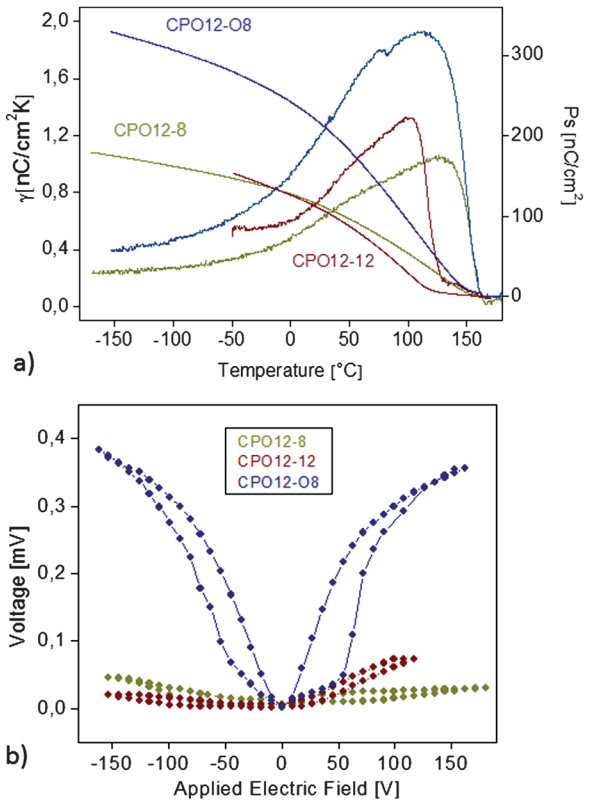

Fig. 5 a) The pyroelectric response and b) the hysteresis loop at 90 °C, for the copolymers.

monomer 12 and 33.69 Å for monomer 8. If we take into account that always at least a half of the copolymers possess either monomer 12 or monomer O12, to calculate the tilt angle of the SmC_2 phase, we use twice the theoretical molecular length for monomer 12 (77.52 Å). These values were taken as a basis for calculating the tilt angle and are summarized in Table 3 for different copolymers exhibiting the smectic C_2 phase. In each case, the averaged interlayer distance was considered with reference to Fig. 4.

The explanation of the interlayer distance and the tilt angle is related to the molecular conformation of the side chains that allows hydrogen bonding between the hydrogen atom in the hydroxyl group and the nitrogen in the azo linkage of the aromatic core. In case of molecules without OH, no interactions with the aromatic core through hydrogen bonding are allowed and the side chains adopt a more relaxed structure, with a small tilt angle and therefore a long interlayer distance.

Table 3 The averaged experimental interlayer distances d and tilt angles β for the copolymers

Copolymer	Interlayer Distance d (Å)	Tilt angle β (°)
CPO12-12	62	36.9
CP8-12	61	38.1
CPO12-8	59	40.4
CPO8-12	58.8	—
CPO12-O8	55.5	44.3

1.5 Physical properties

The pyroelectric measurements (see Fig. 5) were carried out using the modulation pyroelectric technique described in the experimental section and in ref. 15 and 20 according to the simple eqn (1), where T_I is the transition temperature to the isotropic phase:

$$P_s(T) = \int_{T_I}^{T} \gamma(T)dT \quad (1)$$

The poling process was carried out from the isotropic state until room temperature through the liquid crystalline phase. The bias strength was 103 V, at about 10 V μm^{-1} at 20 °C. The external field was removed and the samples were connected to the lock-in amplifier and heated up to few degrees above the isotropic state.

The corrected scale for (γ) and P_s was obtained by comparing the pyroelectric response at a certain temperature with the value measured for a known ferroelectric substance, in this case FLC-397 was used.[21] Three of the five copolymers studied exhibited electric behaviour: CPO12-12, CPO12-8 and CPO12-O8.

The copolymers developed a pyroelectric signal from the glassy state inside the liquid crystalline phase. As can be seen in Fig. 5a the pyroelectric response decreases in the glassy state, producing at the same time an increase in the spontaneous polarization of the material. Also the phase transitions are shifted to lower temperatures. This fact may be indicative of a decrease in the viscosity magnitude of the sample.

The macroscopic polarization calculated using eqn (1) from the obtained pyroelectric signal shows moderate values of polarization from 97 to 30 nC cm^{-2}, at 100 °C and 150 to 275 nC cm^{-2} at −50 °C. These values are slightly lower in comparison with our previous samples. In our Schiff bases composites,[15,16,18] polarization values as high as 400 nC cm^{-2} were reported. The copolymer studied shows typical antiferroelectric loops corresponding to three stable states: one with zero polarization in the absence of the field, and two states with the macroscopic polarization oriented along two possible directions of the external field (see Fig. 5b).

In Fig. 6 the possible disposition of monomers through the main chain is sketched. In the case of CPO12-12, the OH disposition is isotactic, whereas in case of CPO12-O8, more atacticity must be present, which must be responsible for the decrease and the shape of the developed pyroelectric signal (Fig. 5a).

The copolymers CP12-8 and CPO8-12 showed paraelectric behaviour. In the first case this is due to the absence of hydrogen bonding, or a hydroxyl group in the molecule. In the case of CPO8-12, the explanation is the presence of an orthogonal interdigitated SmA phase. SmA phases in liquid crystals have never been described previously as either ferroelectric or antiferroelectric polar phases due to orthogonality in symmetry D_∞. Thus, in CPO8-12, the LC must be a paraelectric phase in which the dipoles are roughly able to orient under an applied electric field but return to their original non polar position once the field is removed.

1.6 Photoresponsive results of copolymers

Differences were noticed depending on the aromatic substitution, which can be easily understood since *ortho* hydroxyl-substituted

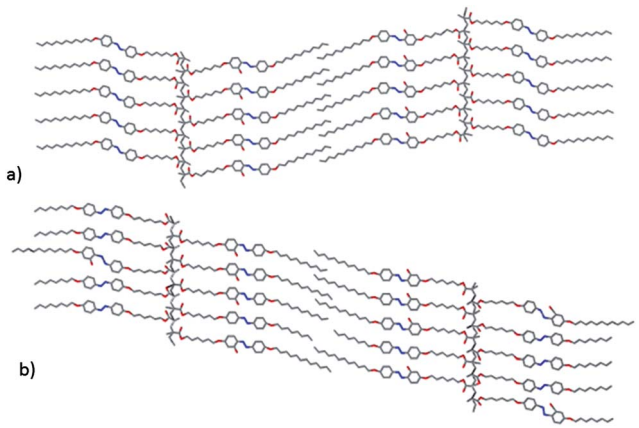

Fig. 6 The anticlinic structure of the bilayered smectic C phase in the copolymers: a) CPO12-12 and b) CPO12-8.

azo-benzenes do not undergo *E–Z* isomerization, but tautomerization due to proton transfer to the corresponding hydrazone, that also is responsible for luminescence observed in these compounds.[22] Attempts to obtain *E–Z* isomerization were unsuccessful under our experimental conditions. Therefore, the phenomena of *E–Z* photoizomerization were studied in THF solutions for these samples without OH like CP12-8 (Fig. 7a and 7b), and for CPO12-8 (Fig. 7c and 7d) partially hydroxylated. The result for copolymer CPO12-12 is not shown here for simplicity but it behaves similar to CPO12-8.

The absorption spectrum of *E*-azo compound groups presents a high intensity σ–σ* transition at 359 nm and a low intensity n–σ* transition at 450 nm. The absorbance near 360 nm decreases significantly to half of its original value after 5 s of irradiation and vanishes after 25 s, while at 450 nm the absorbance increases slightly (see Fig. 7a). On the other hand, a soft change is observed when the isomerization from the *Z* conformation is reversed to *E* by applying light of 450 nm wavelength after 5 min of irradiation (see Fig. 7b), in which the absorbance is half of the initial. This information shows that the effect of reversibility in *E–Z* isomerization can be induced upon visible light irradiation. Nevertheless the amount of *E*-azo compound produced by visible light was much lower than that produced by UV light. This discrepancy must be related to the quantum efficiency of the visible lamp, compared with the UV-vis lamp.

Both absorption spectra show two isosbestic points, at 319 nm and 428 nm, where two absorbent molecules are present in equilibrium. The gradual decrease in absorbance at 359 nm, in the reverse *Z–E* process (Fig. 7b), may be evidence for cycloaddition or isomerization reactions.[23] In the case of the CPO12-12 copolymer, the initial absorption spectra in Fig. 7c showed two peaks with different wavelengths at 361 nm and 376 nm related to monomers 12 and O12 respectively. When irradiated, this copolymer produces a decrease of the peak at 361 nm and

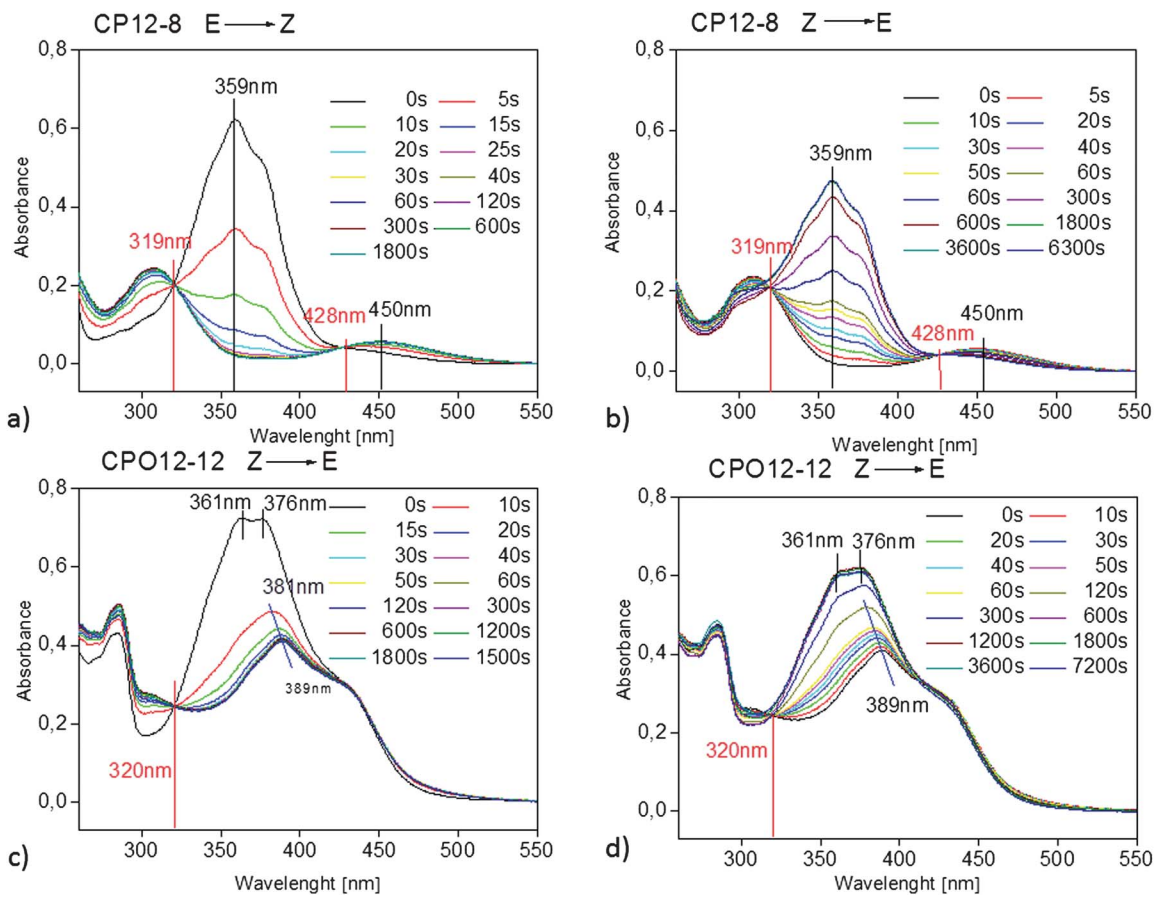

Fig. 7 Changes in the absorption spectra for CP12-8: a) *E* → *Z* and b) *Z* → *E* and CPO12-12: c) *E* → *Z* and d) *Z* → *E*.

a displacement of the 376 nm peak to 389 nm. This last displacement occurs after 1 min of irradiation. This can be also noticed for the return process (Fig. 7d), where the *E*-configuration is conserved until 10 min, reaching an absorbance of 20% less than the initial state. An explanation of this may be due to the amount of OH groups present within the copolymer, thus blocking the *E*–*Z* photo-isomerization. This situation is reproduced for the CPO12-8 copolymer.

The ratio of the *E* and *Z* forms of the azo compounds produced by UV and visible irradiation was determined by means of eqn (2)[23] in the photo stationary state, where A_0 and A_c corresponds to the absorbance at 359 nm before irradiation and at any time during irradiation respectively. When the conversion reaches almost 100%, we can estimate the irradiation time for the full *E*–*Z* isomerization.

$$\% Z = 100(A_o - A_c)/A_o \quad (2)$$

Fig. 8 summarizes the results obtained using this formula for the photoisomerizable copolymers CP12-8, CPO12-8 and CPO12-12 and the corresponding absorptions at several times taken from the experiments carried out in THF solutions.

The percentage of monomer 12 and 8 within the copolymer relates to the % of *Z* obtained when the compounds are irradiated, being a way to calculate the amount of monomer within hydroxyl group in the copolymer. Therefore, we estimate that the copolymers CPO12-8 and CPO12-12 are formed by 60% of monomer 8 and 58% of monomer 12 respectively. These data agree well with the results obtained by means of the ^{1}H-NMR technique.

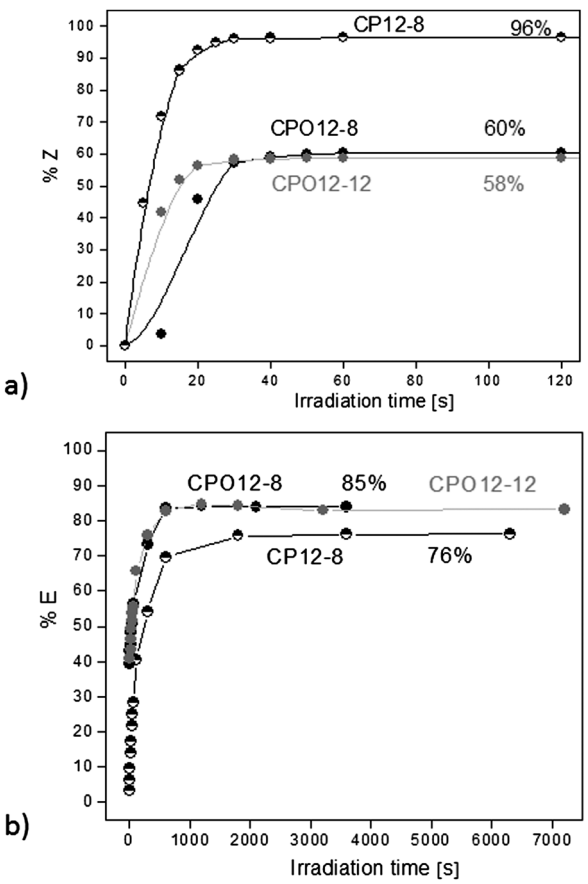

Fig. 8 Irradiation time for the copolymers: a) % of *Z* isomer and b) % of *E* isomer.

Experimental

2.1. Characterizations

The copolymers synthesized were characterized by ^{1}H-NMR spectroscopy using a 300 MHz spectrometer (Bruker, WM 300). The weight, number, and z-average molecular weight $\overline{M_w}$, $\overline{M_n}$, $\overline{M_z}$, $\overline{M_{z+1}}$ and the polydispersity index (PDI) for the copolymers, were determined by gel permeation chromatography (GPC) using a Waters 600 Controller microflow pump, with a Waters 410 Differential Refractometer as the detector. A styragel HT4 (Watters) column, with tetrahydrofuran (HPLC graded) as the eluent with a flow rate of 0.3 ml min^{-1} was used. The material used for calibration was polymethylmethacrylate (PMMA) as the primary standard of the known molecular weight ranging from $\overline{M_w}$ = 5 050 to 280 000 (WAT 035707 and WAT 035706).

The phase transition temperatures for the investigated copolymers were determined using a differential thermal analyzer (Mettler, FP90 DTA). The DTA was calibrated using three different standards: benzophenone (ME18870) m.p. 47.9 ± 0.2 °C; benzoic acid (ME18555) 12.3 ± 0.2 °C and caffeine (ME18872) 236.0 ± 0.3 °C. As a control we used indium (156.6 °C) and a ramp rate of 4 °C min^{-1} (±0.1 K), the same used to carry out the pyroelectric characterization. A polarizing microscope (Leica, DLMP), equipped with a heating stage (HS-1, Instec) was used for temperature dependent investigations of the liquid crystal textures. A video camera (Panasonic, WVCP414P) installed on the polarizing microscope allowed for real time image capture, *via* coupling with a video capture card (Miro DC-30). The samples were supported between glass plates.

For obtaining the pyroelectric signal (γ), the copolymers were confined in cells of 8 μm thicknesses at the isotropic phase for capillarity. The cells were placed inside a temperature controlled thermal oven (Linkman THMSE 600) that allows a temperature rate control range from 0.1 °C min^{-1} up to 20 °C min^{-1}. To achieve a low temperature, an external cooling system (temperature regulated cooler Linkman CI93 and Linkman LND) was used. The variable temperature pulses were applied to the samples using modulated light from a semiconductor laser (λ = 685 nm, P = 27 mW, modulation capability from DC to 5 MHz) fed by a 5 V DC power supply. The 70 Hz modulation frequency was regulated by a lock-in amplifier (EG&G Model T260 DSP) and the form of the signal was obtained using a 2-channel oscilloscope (Hewlett Packard 54600A operating at 100 MHz).

The pyroelectric response from poled samples was measured as a sine voltage with the lock-in amplifier. To make the poling process an external DC supply was used (100 V). The obtained signals were acquired with a computer that is connected to the lock in amplifier and further processed by appropriate software. When the material is pyroelectric, the application of an electric field reverses the direction of spontaneous polarization showing one induced phase transition in antiferroelectric material as a double hysteresis loop.

X-Ray measurements were carried out using Cu-Kα radiation; the samples were contained in 0.8 mm glass capillaries (Lindemann) held in a copper block. The precise data for aligned samples in the small angle region were performed by focusing a horizontal two-circle X-ray diffractometer (STOE STADI 2) with a linear position-sensitive detector for data collection. The temperature was stabilized within the range of 30 °C to 170 °C ± 0.1 °C during the measurements.

The UV-vis spectra in THF solution were recorded in an ATI Unicam UV/Vis Spectrometer UV3. The light source for photoirradiation was a 450 W medium pressure mercury lamp (B100 AP) for $Z \rightarrow E$ isomerization (450 nm) and a commercial dichroic lamp of 50 Watts (360 nm) for E–Z isomerization. In the first case, a bandwidth filter with two specific wavelengths at 366 nm and 746 nm (50.27% and 9.47% transmittance) was used. In the second case, a visible filter was used, with a cut off at 392 nm (80–89% transmittance). This study was realized for the samples CP12-8, CPO12-12 and CPO12-8.

2.2. Materials

Different mixtures between the monomers O12, O8, 12, and 8 were utilized to obtain the five copolymers. The concentration of azo-benzene monomers with and without OH present in the copolymer was determined by ^{1}H-NMR and UV measurement in THF solution (see Fig. 8).

The copolymerization was performed under nitrogen in sealed bottles. The CPO12-8 copolymer was synthesized mixing O12 (0.25 g, 0.44 mmol) and monomer 8 (0.25 g, 0.50 mmol) in dry toluene (5 mL) using AIBN as an initiator at 60 °C for 48 h. Afterward, the reaction mixture was precipitated in cold acetone and the collected copolymer was dried under reduced pressure. All the copolymers used for further study in this paper were realized using the same technique described in literature.[14]

CPO12-8 ^{1}H-NMR ($CDCl_3$) δ (ppm): 13.51 (s, 1H, Ar(**OH**)–N=N–), 7.72 (d, 4H, N=N–Ar**H**), 7.59 (m, 3H, N=N–Ar**H**; –Ar(OH)**H**–N=N–), 6.82 (dd, 6H, –Ar**H**–N=N–Ar**H**; –Ar(OH)–N=N–Ar**H**), 6.41 (d, 1H, Ar(OH)**H**–N=N–), 6.27 (d, 1H Ar(OH)**H**–N=N–), 3.83 (O–C**H$_2$**–); 1.69–1.18 (–C**H$_2$**–),0.81 (t,6H, –C**H$_3$**–).

CPO12-O8 ^{1}H-NMR ($CDCl_3$) δ (ppm): 13.50 (s, 1H, Ar(**OH**)–N=N–), 7.58 (m, 3H, N=N–Ar**H**; –Ar(OH)**H**–N=N–), 6.80 (d, 2H, –N=N–Ar**H**), 6.41 (d, 1H, Ar(OH)**H**–N=N–), 6.27 (d, 1H, Ar(OH)**H**–N=N–), 3.81 (O–CH_2–); 1.67–1.18 (–CH_2–), 0.81 (t, 3H, –CH_3–).

CPO12-12 ^{1}H-NMR ($CDCl_3$) δ (ppm): 13.57 (s, 1H, Ar(**OH**)–N=N–), 7.72 (d, 4H, N=N–Ar**H**), 7.59 (m, 3H, N=N–Ar**H**; –Ar(OH)**H**–N=N–), 6.84 (dd, 6H, –Ar**H**–N=N–Ar**H**; –Ar(OH)–N=N–Ar**H**), 6.46 (d, 1H, Ar(OH)**H**–N=N–), 6.31 (d, 1H, Ar(OH)**H**–N=N–), 3.87 (O–C**H$_2$**–); 1.67–1.18 (–C**H$_2$**–), 0.81 (t, 6H, –C**H$_3$**–).

CPO8-12 ^{1}H-NMR ($CDCl_3$) δ (ppm): 13.51 (s, 1H, Ar(**OH**)–N=N–), 7.73 (d, 4H, N=N–Ar**H**), 7.58 (m, 3H, Ar(OH)–N=N–Ar**H**; –Ar(OH)**H**–N=N–), 6.85 (dd, 6H, –Ar**H**–N=N–Ar**H**; –Ar(OH)–N=N–Ar**H**), 6.41 (d, 1H, Ar(OH)**H**–N=N–), 6.28 (d, 1H, Ar(OH)**H**–N=N–), 3.89 (O–C**H$_2$**–); 1.67–1.18 (–C**H$_2$**–), 0.80 (t, 3H, –C**H$_3$**–).

CP8-12 ^{1}H-NMR ($CDCl_3$) δ (ppm): 7.73 (dd, 4H, N=N–Ar**H**), 6.83 (dd, 4H, Ar**H**–N=N–), 3.83 (O–CH_2–); 1.66–1.18 (–CH_2–), 0.81 (t, 6H, –CH_3–).

The yields of the copolymers were 50%, except for the CP8-12, that presented only a yield of 25%.

Conclusions

The copolymers CPO12-8, CPO12-12 and CPO12-O8 show an antiferroelectric behaviour that is reasonable to expect due to the intrinsic properties of the polymer PM6OA12[17] always present in these samples. In the case of CPO12-O8 the observed antiferroelectricity has to do with the formation of bilayered smectic C_2 phases and the hydrogen bonding at the polymeric matrix that is built in the mesophase constructing the anti-clinic phase.[14,15]

In case of CPO12-8 and CPO12-12 a new molecule association is allowed due to the OH distribution preferably just at one side of the bilayer smectic phase. Here syndiotacticity of the side chain distribution to each side of the main chain plays an important role to build a polar mesophase.

The CP12-8 and CPO8-12 copolymers showed paraelectric behaviour. The reason why they do not build polar mesophases is due to the absence of hydrogen bonding in the case of CP12-8. For the other sample, the orthogonal interdigitated SmA restricts the possibility of a polar structure since in the case of liquid crystals, due to symmetry considerations this mesophase has never been reported as polar, and therefore is a well-known paraelectric phase.

Copolymers without hydroxyl groups like CP12-8, give reversible E–Z isomerization induced by UV and visible irradiation. In the case of CPO12-12 and CPO12-8 copolymers, they go easily from E to Z but the reverse is hardly affected by the non-isomerizable component always present in the copolymer.

Acknowledgements

C. M. González-Henríquez acknowledges a scholarship from Conicyt and E. A. Soto-Bustamante is grateful for financial support from Project FONDECYT 2007 Nr. 1071059, Merck Chile S.A. and VID, Universidad de Chile.

References

1 R. B. Meyer, L. Liebert, L. Strzelecki and P. Keller, *J. Physique Lett.*, 1975, **36**, 69.
2 A. Mori, K. Katahira, K. Kida and H. Takeshita, *Chem. Lett.*, 1992, 1767.
3 A. Mori, K. Hirayama, N. Kato, H. Takeshita and S. Ujiie, *Chem. Lett.*, 1997, 509.
4 R. Zentel, *Angew. Chem.*, 1989, **101**, 1437.
5 M. Brehmer, R. Zentel, G. Wagenblast and K. Siemensmeyer, *Macromol. Chem. Phys.*, 1994, **195**, 1891.
6 M. Brehmer and R. Zentel, *Macromol. Rapid Commun.*, 1995, **16**, 659.
7 I. Benne, K. Semmler and H. Finkelmann, *Macromolecules*, 1995, **28**, 1854.
8 M. Brehmer, R. Zentel, F. Gießelmann, R. Germer and P. Zugenmaier, *Liq. Cryst.*, 1996, **21**, 589.
9 E. Gebhard and R. Zentel, *Macromol. Chem. Phys.*, 2000, **201**, 902.
10 S. U. Valerien, F. Kremer, E. W. Fischer, H. Kapitza, R. Zentel and H. Poths, *Makromol. Chem. Rapid Commun.*, 1990, **11**, 593.
11 H. Kawai, *Jpn. J. Appl. Phys.*, 1969, **8**, 975.
12 K. EL-Hami, M. Hara, H. Yamada and K. Matsushige, *Ann. Chim. Sci. Mater.*, 2001, **26**, 217.

13 E. A. Soto Bustamante, S. V. Yablonsky, L. A. Beresnev, L. M. Blinov, W. Haase, W. Dultz, and Yu. G. Galyametdinov, "Methode zur Herstellung von polymeren pyroelektrischen und piezoelektrischen Elementen", DE 195 47 934.3, 20.12.95; EP 0 780 914, 25.06.97; JP 237921/907 09.09.97; US 5 833 833, 10.11.98.
14 E. A. Soto-Bustamante, S. V. Yablonsky, B. I. Ostrovskii, L. A. Beresnev, L. M. Blinov and W. Haase, *Chem. Phys. Lett.*, 1996, **260**, 447.
15 E. A. Soto-Bustamante, D. Saldaño-Hurtado, R. O. Vergara-Toloza and P. A. Navarrete-Encina, *Liq. Cryst.*, 2000, **30**, 17.
16 C. M. González-Henríquez, E. A. Soto-Bustamante, D. A. Waceols-Gordillo and W. Haase, *Liq. Cryst.*, 2009, **36**, 541.
17 E. A. Soto-Bustamante, P. A. Navarrete Encina, T. Weyrauch and R. Werner, *Ferroelectrics*, 2000, **243**, 125.
18 C. M. González-Henríquez, E. A. Soto-Bustamante, R. O. Vergara-Toloza and W. Haase, *Chem. Phys. Lett.*, 2011, **510**, 212.
19 E. A. Soto Bustamante, S. V. Yablonskii, B. I. Ostrovskii, L. A. Beresnev, L. M. Blinov and W. Haase, *Liq. Cryst.*, 1996, **21**, 829.
20 S. Hiller, L. A. Beresnev, S. A. Pikin and W. Haase, *Ferroelectrics*, 1996, **180**, 153.
21 R. Nurmukhametov, D. N. Shigorin, Y. Kozlov and V. A. Puchkov, *Opt. Spectrosc.*, 1961, **11**, 327.
22 C. Kyung-Soo, K. Hyun-Wuk, K. Yong-Bae and K. Jong-Duk, *Liq. Cryst.*, 2004, **31**, 639.
23 L. Cui, Y. Zhao, A. Yavrian and T. Galstian, *Macromolecules*, 2003, **36**, 8246.